Modeling Assessment of 2017 Prescribed Grassland Burning in the Flint Hills Region

EPA-454/R-21-004
June 2021

Modeling Assessment of 2017 Prescribed Grassland Burning in the Flint Hills Region

U.S. Environmental Protection Agency
Office of Air Quality Planning and Standards
Air Quality Assessment Division
Research Triangle Park, NC

U.S. Environmental Protection Agency
Region 7
Air and Radiation Division
Lenexa, KS

1. BACKGROUND

Prescribed and wild grassland burning results in emissions of pollutants that can react in the atmosphere to become particulate matter less than 2.5 microns in diameter and ozone (Baker et al., 2019), both of which have known negative health effects in humans (Reid et al., 2016) and are regulated under the Clean Air Act with National Ambient Air Quality Standards. Other pollutants emitted by grassland fires are toxic (e.g., formaldehyde, mercury) or have negative ecological impacts (e.g., ammonia, SO2, NOX) and potentially contribute to impaired visibility in downwind areas including National Parks and National Monuments.

The Flint Hills ecoregion contains approximately 5 million acres of grassland (Baker et al., 2019). Each year when weather is conducive, hundreds of thousands of acres are burned with prescribed fire to minimize the encroachment of woody growth, maintain the ecosystem for native species, and to promote agribusiness (Towne and Craine, 2016; Weir and Scasta, 2017). A fire interval of 1 to 3 years is considered necessary to minimize encroachment of woody vegetation (Ratajczak et al., 2016).

There are over 5 million acres of grassland in the Flint Hills region (Baker et al., 2019) which must be burned every 1 to 3 years to meet ecosystem resilience (Ratajczak et al., 2016), however only a fraction of the region is burned on this frequency (Baker et al., 2019). Prescribed fire activity in this region is largely done within a few weeks period from late March to mid-April each year (Baker et al., 2019). The large amount of activity on a given day has led to downwind areas exceeding the level of the O3 National Ambient Air Quality Standard (NAAQS). The state of Kansas implemented a smoke management plan in 2010 to encourage prescribed burning practices that minimize the emissions of pollutants that can react in the atmosphere to form O3 (Kansas Department of Health and Environment, 2010). If prescribed fire was done over the longer dormant season rather than focusing on a few weeks in the early spring season more acres could be burned, and air quality impacts would likely be less on any given day (Weir and Scasta, 2017).

Complex photochemical grid models have been used to demonstrate grassland burning impacts on secondarily formed pollutants (e.g. O3, PM2.5, regional haze) to support retrospective regulatory assessments (Baker et al., 2016; Kansas Department of Health and Environment, 2012). Photochemical grid models have historically underestimated regional PM2.5 organic aerosol (Wagstrom et al., 2014), which is the largest component of biomass burning PM emissions. Photochemical models have been shown to replicate downwind surface level elevated PM2.5 impacts for large western wildfires (Baker et al., 2016; Baker et al., 2018), but systematically over-predict at monitors downwind of grassland burning in the Flint Hills region (Baker et al., 2016). These models tend to systematically overestimate O3 at monitors downwind of both wild (Baker et al., 2016; Baker et al., 2018) and grassland fires (Baker et al., 2016).

In March and November 2017, a field study took place in the Flint Hills region to better understand prescribed grassland fire fuels, emissions, and their impacts on air quality in the ecoregion (Whitehill et al., 2019). The study included an extensive cataloging of fuel characteristics surveyed during individual burns and ceilometer deployment to assess smoke plume heights. In this work, we use the unique dataset collected during the 2017 Flint Hills study to constrain and evaluate simulations of the observed burns in the Community Multi-scale Air Quality (CMAQ) modeling system. We also evaluate local to regional scale model-predicted smoke transport using other datasets including satellite imagery and meteorological observations from surface and sonde measurements. The combination of co-located fuel data and atmospheric observations collected during the 2017 Flint Hills study provides an opportunity to assess air quality model skill in representing different scales of prescribed grassland fire smoke transport in the region.

Here, the Community Multiscale Air Quality Model (CMAQ) was applied for specific prescribed grassland fires in the Flint Hills region in 2017 instrumented with surface and remotely sensed measurements and entire prescribed burning seasons to illustrate how well the model predicts regional air quality compared with routine surface monitors and space-based air quality products. The influence of grid resolution was explored for the 2017 case studies and a common regulatory assessment grid resolution was used for the longer-term seasonal evaluation. The entire record of prescribed fires at Konza Prairie in 2017 and 2018 are compared with the HMS satellite detection product to evaluate burn detection location accuracy for these types of grassland fires.

2. METHODS

Field measurements were made near multiple prescribed grassland fires at Konza Prairie in March and November of 2017 and at Tallgrass Prairie in November of 2017 (Whitehill et al., 2019). Table 1 shows the date, size, fuel load, and fuel moisture measured for prescribed burns at both locations. Dominant fuel types were identified, and fuel load was estimated for these prescribed fires as part of the field study effort. Fuel moisture and other meteorological data were determined using nearby routine measurement networks. As part of this field study, a ceilometer was operated continuously at Konza Prairie during March, a period of increased fire activity in the region (Baker et al., 2019), to capture local to regional scale prescribed grassland fire impacts. The ceilometer was operated again in November 2017 at Konza Prairie for a similar objective then deployed at Tallgrass Prairie to capture local scale impacts by being placed immediately adjacent and downwind of a single large prescribed fire (11/15/17). A second ceilometer was operated during November 2017 at the Tallgrass Prairie Visitor Center upwind of the prescribed fire to provide an estimate of incoming aerosol and the surface mixing layer height.

Model configuration and application

Models were applied for the entirety of the March and November 2017 periods coincident with a field study ceilometer deployment in the region. The extent of the continental scale 12 km domain, 4 km domain covering the Kansas and northern Oklahoma, and inner 1 km domains over a portion of the Flint Hills are shown in Figure 1. The springtime 1 km modeling domain was centered over the Konza Prairie Biological Station and was extended in the November modeling simulation to encompass the Tallgrass Prairie National Preserve.

Figure 1. Spatial extent covered by the 12, 4, and multiple 1 km model domains with gradients representing grassland coverage. The Flint Hills ecoregion is shown with the dashed black outline. Ceilometer placement at Konza Prairie and Tallgrass Prairie (co-located RAWS surface meteorological site) are also shown.

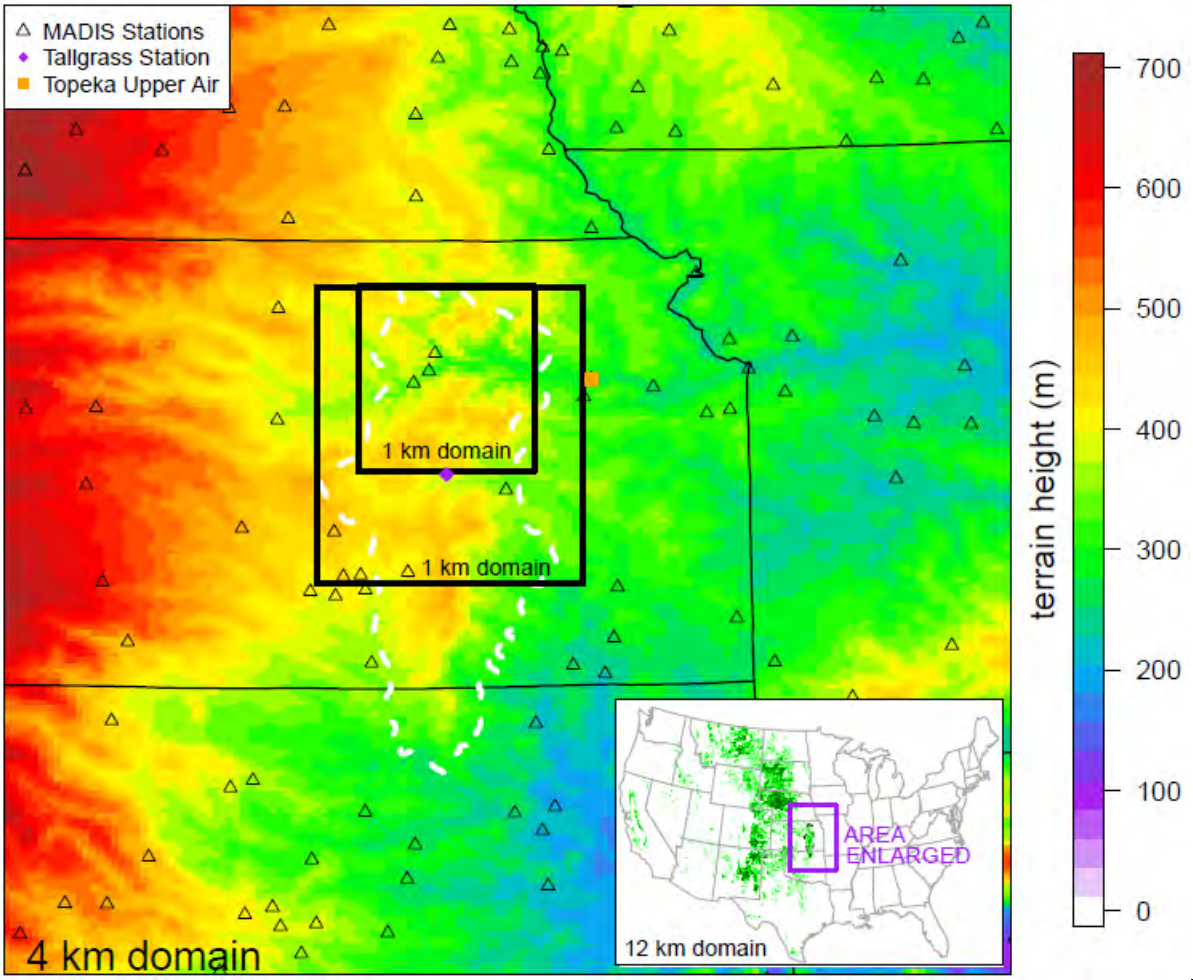

Meteorological model simulations over the Flint Hills region were completed using version 3.9 of the Weather Research and Forecasting (WRF) model with the Advanced Research dynamical core (Skamarock et al., 2005). Table 1 summarizes the WRF model set-up, where the model configuration consisted of three one-way nested domains with horizontal grid spacing of 12, 4 and 1 km and 35 vertical levels. The vertical atmosphere was resolved using 35 vertical layers with the lowest 12 levels within approximately 1 km of the surface.

WRF physics options used in the simulations include the Rapid Radiative Transfer Model longwave and shortwave radiation schemes (Iacono et al., 2008) and the Thompson (Thompson et al., 2008) microphysics scheme. The Teidke cumulus parametrization (Tiedtke, 1989) was applied in the 12-km domain and no cumulus parametrization was used in the inner 4 km and 1 km domains. Each simulation used the Mellor–Yamada–Janjic (MYJ) PBL scheme and Monin-Obukhov (Janjic Eta) similarity surface layer scheme. The United States Geological Survey (USGS) land use data set was used along with the NOAH land surface model to simulate soil moisture and temperature (Niu et al., 2011). The 12 km resolution North American Mesoscale model (NAM) operational analyses was used to initialize

atmospheric and land surface variables as well as provide the lateral boundary conditions. WRF simulations were executed using 5.5 day overlapping run segments.

Table 1. Configuration options selected for the WRF model applications.

Model Feature	Description
Version	3.9
Boundary Conditions	NAM Analysis
Vertical Levels	35
Model Top	50 hPa
Domains	3 one-way nests
Resolution	12 km, 4 km, 1 km
Number of Grid Cells	12 km (471 x 312), 4 km (271 x 325), 1 km (100 x 140 -- spring; 161 x 233 -- November)
Timestep (s)	36, 12, 3
Planetary Boundary Layer	Mellor–Yamada–Janjic (MYJ)
Surface Layer	Monin-Obukhov (Janjic Eta)
Land Surface	NOAH
Land Use	USGS
Radiation	RRTMG
Microphysics	Thompson
Cumulus	Tiedke, 1989; None for 4 km or 1 km domains

Gases and aerosol were predicted with the Community Multiscale Air Quality (CMAQ) version 5.3 model. The Carbon Bond version 6r3 was used to represent gas phase chemistry (Emery et al., 2015), ISORROPIA II inorganic particulate partitioning (Fountoukis and Nenes, 2007), and aqueous phase chemistry (Fahey et al., 2017). Biomass burning consists of high molecular weight compounds and has extremely low volatility (Washenfelder et al., 2019) so organic aerosols were treated as non-volatile. Some anthropogenic and biogenic VOC yield secondary organic aerosol and were treated as semi-volatile (Carlton et al., 2010).

Fire location and timing were based on HMS fire detections coupled with burn area products reconciled with the SmartFire2 (SF2) system. Emissions were based on fuel type and loading from the Fuel Characteristic Classification System (FCCS) Fuel Loading Module version 2 and fuel consumption from the CONSUME module of the BlueSky Framework version 3.5.0 (rev 38169) (Larkin et al., 2014). The Fire Emission Production Simulator Module (FEPS) version 2 and fuel moisture estimates from the Wildland Fire Assessment System (WFAS), each of which are also part of the same BlueSky system, were used in the process of calculating emissions from the fires.

Plume rise was estimated with the modified Briggs approach, which has been used extensively to estimate local to regional scale smoke transport from prescribed fires in the Flint Hills region (Baker et al., 2016), Pacific northwest (Zhou et al., 2018), and wildfires in California (Baker et al., 2018) and Arizona (Baker et al., 2016). Plume height is a function of the buoyant heat flux, which is based on acres burned, fuel loading, and the duration of the fire (Zhou et al., 2018). Prescribed burns measured as part of the field study were modeled using actual burn unit size in addition to the default approach.

The emissions modeling process used here assigns the same allocation of daily emissions to specific hours of the day for all prescribed fires. The default profile applied to prescribed fire in SMOKE allocates

most emissions in hours 11 am to 6 pm (Baker et al., 2016), which generally matches prescribed burning activity in this region (Baker et al., 2019) but does not accurately reflect start time and duration of individual fires that typically burn for less than 4 to 6 hours (Brey et al., 2017). Prescribed burns measured as part of the field study were modeled using actual start and end times in addition to a second simulation that used the default hour of the day allocation profile (Figure A1).

CMAQ was applied using the SF2/BlueSky system and separate sensitivity simulation where prescribed burns measured as part of the field study were modeled using actual acres burned, fuel loading, fuel consumption, and timing information. A third simulation without prescribed grassland fires was done to compare against the runs with prescribed fire to isolate the impacts of these emissions on predicted air quality (Kelly et al., 2015).

Surface and Sonde Measurements

The Flint Hills WRF simulations were evaluated using surface meteorological observations obtained from NOAA's Meteorological Assimilation Data Ingest System (MADIS) dataset. Meteorological measurements were compared with model estimates of 2 m temperature and humidity, and 10 m winds (Figure 1). Additionally, a Remote Automated Weather Station (RAWS) located at Tallgrass Prairie provided solar radiation, fuel moisture, and precipitation measurements along with surface temperatures, humidity and winds. Vertical profiles of temperature and wind from rawinsondes released daily in the morning and evening from the Topeka airport were used to evaluate the model's ability to reproduce the vertical structure of the boundary layer.

Remote Sensing Measurements and Imagery

Vaisala ceilometers (CL31 and CL51) were episodically deployed at locations in the Flint Hills ecoregion in March and November 2017 (Figure 1) to provide a near-continuous (approximately 36 s interval) backscatter profile measurements up to 4.5 km. BL-View software was used to calculate aerosol layer heights and cloud base heights from the backscatter profiles. The aerosol layer determination is based on a gradient method that identifies steep decreases within the backscatter profile, with the first negative gradient maximum identified as the boundary layer height. Boundary layer heights were temporally aggregated to 5 min averages and periods were excluded from this analysis when the standard deviation exceeded 0.20 km or relative standard deviation (standard deviation divided by the mean) exceeded 20% (Knepp et al., 2017). A Campbell Scientific ceilometer was operated during the November 15 burn at Tallgrass Prairie and located upwind of the prescribed fire.

Satellite true color imagery products from Moderate Resolution Imaging Spectroradiometer (MODIS) provide information about clouds and smoke in the region (www.airnowtech.com). Images from the terra satellite represent ~10:30 am local time and aqua satellite images represent ~1:30 pm local time. Level 1 and 2 measurements of AOD were obtained from the Aerosol Robotic Network (AERONET; aeronet.gsfc.nasa.gov) site located at Konza Prairie.

Field measurements: biomass type, biomass sampling

Biomass was collected from 1 m^2 sized clip plots at Konza Prairie Biological Station burn units in March (N=3) and November (N=1). A total of 10 replicants were collected, dried, and weighed from 3 large burn treatment areas and 5 replicants for a smaller treatment area. An average was calculated for each of the burn treatments. Dominant vegetation species were identified by an ecologist. Fuel moisture was

collected hourly at a RAWS located at Tallgrass Prairie (https://mesowest.utah.edu/cgi-bin/droman/meso_base.cgi?stn=TGSK1&time=GMT).

3. RESULTS & DISCUSSION

Fire location and detection, fuel type, fuel loading

A total of 13 prescribed fires (Table 2) were observed as part of the field study, each with different timing and size. The modeling system was able to correctly place most of the prescribed fires observed during the field study based on satellite fire detections on days without cloud cover (9 days). Only 3 of the prescribed fires were not detected by satellite on cloud-free days and each of these totaled less than 100 acres and were not active during the overpass time of a polar orbiting satellite. Missed detection of prescribed fire will result in an underestimate of emissions unless other sources of information provide the location, date, and area burned. Regional prescribed fire was minimal during the fall period, although large prescribed fires occurred at Tallgrass Prairie on November 13th (~2000 acres) and 15th (~1000 acres). Cloudy conditions on November 13th precluded satellite detection. It is possible more prescribed fire activity happened in the spring but was not detected by satellites due to extensive periods of cloud cover over the region.

Table 2. Burn unit and fuel information for prescribed fires at Konza Prairie and Tallgrass Prairie in 2017 observed as part of the field study. All fuel moisture measurements were from a Tallgrass Prairie monitor location.

Site	Burn	Date	Burn Unit Size (acres)	Approx. Start Time	Approx. End Time	HMS detected	Measured Total Fuel Loading (tons/acre)	FCCS Total Fuel Loading (tons/acre)	Percent Difference in PM emissions	Measured Daily Avg. Fuel Moisture (%)	WFAS 10-hr Fuel Moisture (%)	WFAS Live Fuel Moisture (%)	WFAS Duff Fuel Moisture (%)	Percent Difference in PM emissions
Konza	1	3/15/2017	111	13:30	17:15	Cloud	3.10	3.96	-8%	116	60	130	150	-14%
Konza	2	3/16/2017	84	10:50	12:00	No	2.36	4.08	-48%	90	60	130	150	48%
Konza	3	3/16/2017	205	13:00	14:30	Yes	2.78	4.08	-38%	90	60	130	150	48%
Konza	4	3/17/2017	11	15:00	16:00	Cloud	3.10	3.96	-8%	128	60	130	150	-15%
Konza	5	3/17/2017	16	16:40	17:15	Cloud	3.10	4.08	-31%	128	60	130	150	40%
Konza	6	3/20/2017	294	10:45	15:30	Yes	2.68	4.08	-41%	90	60	130	150	48%
Konza	7	3/20/2017	335	10:45	15:30	Yes	2.68	4.08	-41%	90	60	130	150	48%
Konza	8	3/20/2017	299	10:45	15:30	Yes	2.36	4.08	-48%	90	60	130	150	48%
Konza	9	3/20/2017	148	10:45	15:30	Yes	2.36	4.08	-48%	90	60	130	150	48%
Konza	10	11/10/2017	27	13:50	14:45	No	4.97	4.08	10%	101	60	130	150	46%
Konza	11	11/10/2017	26	15:30	16:15	No	4.97	4.08	10%	101	60	130	150	46%
Tallgrass	12	11/13/2017	1,960	10:30	16:30	Cloud	2.40	4.08	-47%	193	60	130	150	6%
Tallgrass	13	11/15/2017	938	12:00	16:00	Yes	2.40	4.08	-47%	175	60	130	150	21%

Fuels at each location were largely cheatgrass (Bromus tectorum), Indian grass (Sorghastrum nutans), big bluestem (Andropogon gerardii), and little bluestem (Schizachyrium scoparium). The FCCS fuel type matched these at each burn unit (Table 2). Burns 1 and 4 were categorized as “old field grassland” resulting in a slightly different fuel loading and type (more shrubs) than the other locations. Fuel loading estimated by FCCS and field-based data for each burn are shown in Table 2. Fuel loading estimates based on FCCS for these prescribed fires tended to be higher (35% on average) than the field data but varied for each burn unit (-18% to 73%).

Figure 2 shows satellite burn detections and burn areas at Konza Prairie for multiple days from 2017. The prescribed fires during 2017 were often partially or fully obscured by cloud cover. The March 16 and 20 burns had clear skies. Extensive prescribed fire activity across the region on April 11 may have obscured the actual fire from detection and resulted in many false detections outside the burn unit. Some of the missed prescribed burns may be the result of size and timing of the fire missing satellites with higher resolution detection products. Only one of the 2 days of prescribed fire at Tallgrass Prairie

was captured by satellite due to extensive cloud cover on the first day (Figure 2). A similar analysis was done for burn days at Konza Prairie in 2018 to capture additional periods of clear skies (Figure A2). Most of the 2018 prescribed fires at Konza Prairie were detected with a least one satellite detection within a km of the actual burn unit (Figures LOCATION-KONZA).

Figure 2. Satellite detected fires based on the HMS system (red) and burn areas (green outline) by day at Konza Prairie (blue outline) for 2017. Gray shading represents grassland coverage at 1 km grid spacing.

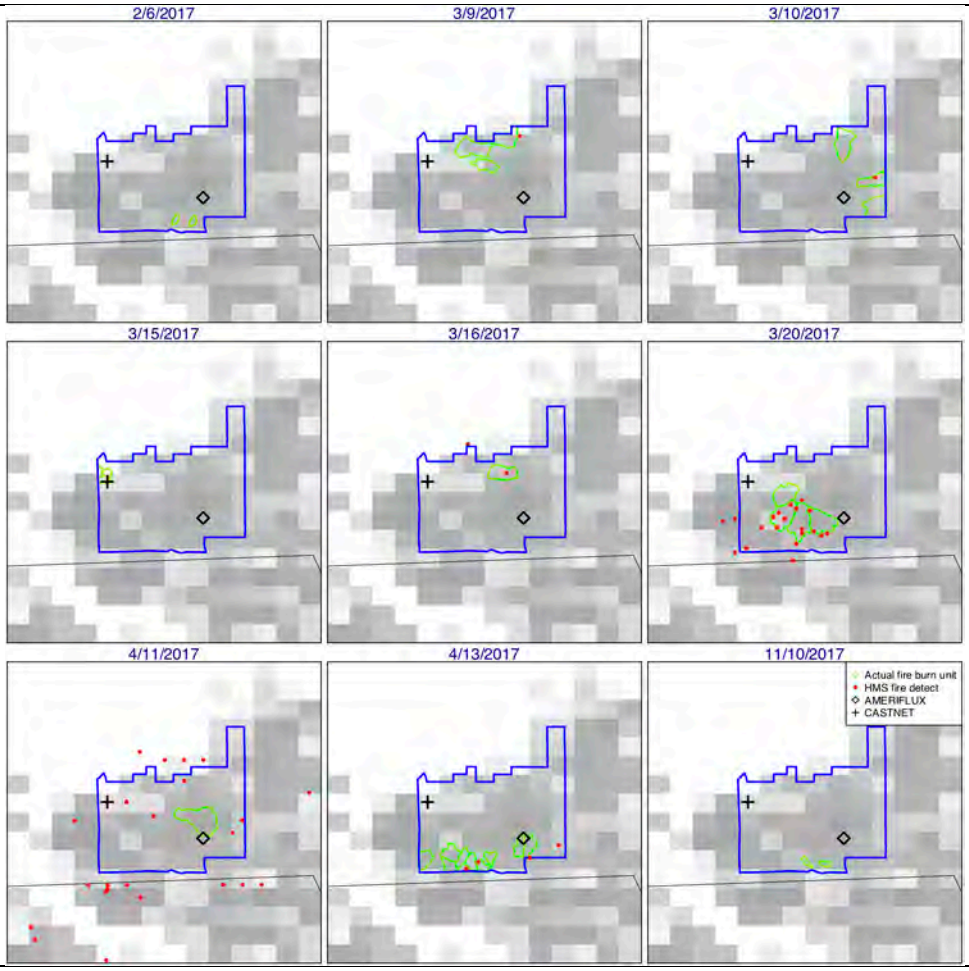

Fuel moisture

Fuel moisture was estimated for 10-hr fuel (shrubs), live fuel (grasses), and duff (litter) as 60, 130 and 150 (% of 1,000 hr fuel) at each of the burns by the WFAS system. Daily average fuel moisture data measured at Tallgrass Prairie is provided in Table 2 for each prescribed fire. Fuel moisture can exceed 100% due to water in the fuel that may weigh more than the dry fuel. The WFAS climatological data tended to be higher for live fuel and duff than measured during the spring and lower in the fall for the days that were part of the field study at Konza Prairie and Tallgrass Prarie. Applying CONSUME with the day specific fuel moisture resulted in drier fuel, more consumption, and higher emissions (40 to 48%) during the spring burn units dominated by grass and duff. Burn units dominated by shrubs had less consumption and emissions because measured fuel moisture levels for 10-hr fuel were higher than the WFAS estimate. The larger burn units at Tallgrass Prairie had much less change in fuel consumption and

emissions (increases of 6 to 21%) compared to the smaller units at Konza Prairie despite the higher fuel moisture measured compared to WFAS. For the prescribed fires considered here, fuel loading overestimates by FCCS and fuel moisture overestimates from WFAS tend to compensate in terms of resulting emissions, which would decrease with more accurate fuel loading information (by 44% on average) and increase for these particular burns based on the fuel being drier which would typically lead to more consumption and emissions (by 39% on average).

Timing

The approximate start and end times for specific fires were recorded for 5 separate prescribed fires from 2017 (Figure 3). These prescribed fires ranged in size (26 to 1,960 acres), start time (mid-morning to late afternoon), and duration (less than an hour to 6 hours). All fires finished burning before dusk. A strong linear relationship (r^2=.88, residual error=0.88 and p=0.0058) exists between the fire duration and acres burned (Figure 2). Including fuel loading results in a slightly better estimate of total fire duration (r^2=.97, residual error=0.46, p=0.0058). The sample size is small (N=5), but these data suggest that fire duration could be estimated based on acres burned and fuel loading. Satellite data indicate prescribed burns in this region typically start mid-morning or after lunch (Baker et al., 2019) and last up to 6 hours (Brey et al., 2017).

Figure 3. Default (red trace) and actual prescribed grassland fires included in a field study at Konza Prairie and Tallgrass Prairie in 2017. The inset shows area burned and burn duration for a subset of the prescribed fires with well characterized start and end times.

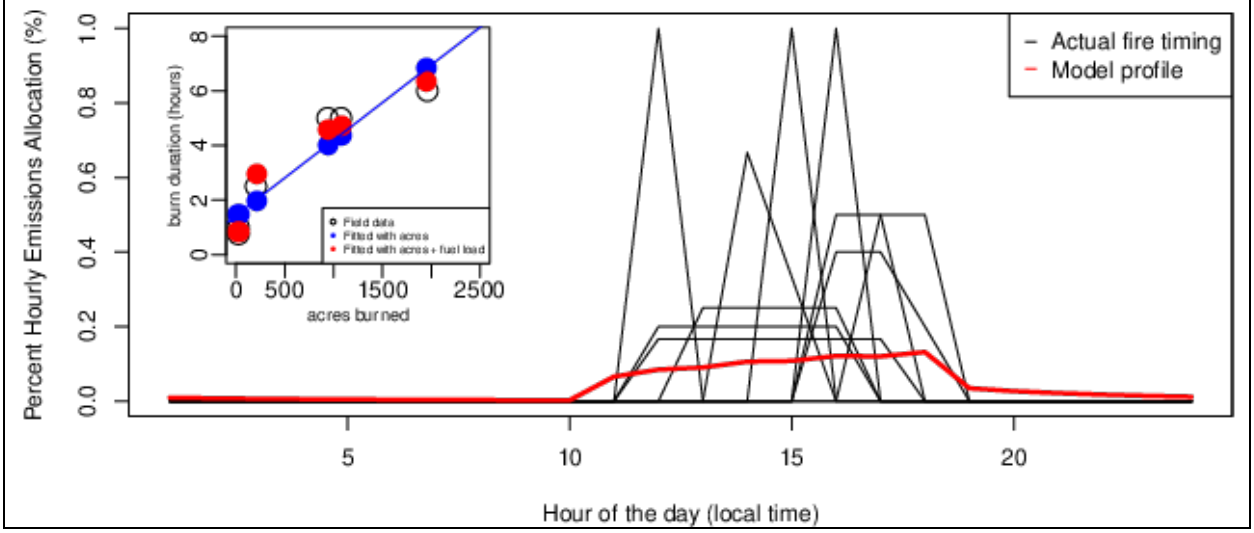

Since prescribed fires in this region are often short in duration and small in size, satellite products may not always have start and end time estimates. This means that the linear equations could provide an estimate of duration when coupled with a generic start time of late morning for longer fires and early afternoon for shorter fires. Currently, emissions are allocated to daytime hours, with most between 11 am and 6 pm (Figure A1) (Baker et al., 2016). The default assumption for prescribed fire duration was longer than even the largest fires observed during the field study. Overestimating burn duration will result in lower hourly heat flux and less plume buoyancy, which can result in less realistic plume heights (Zhou et al., 2018). In the future, fire-specific temporal profiles could be incorporated into an emissions processing system by using the fire size and time of detect for those fires detected by satellite.

November 15, 2017 case study (Vertical plume placement)

Multiple ceilometers were operated at Tallgrass Prairie on November 15, 2017. One ceilometer was placed to capture smoke impacts immediately downwind of the prescribed fire and the other upwind at the Tallgrass Prairie Visitors Center to characterize aerosol inflow and aerosol layer structure (Figure 4). The second ceilometer operated upwind and shows very little aerosol loading in the area. Based on the vertical backscatter gradient at the upwind ceilometer, the data suggest that the surface mixing layer was between 1000 and 1200 meters during the prescribed fire (Figure 5). The prescribed fire started around 12:30 pm along the southern edge of the burn unit which was close to the downwind ceilometer. The fire progressed to the north while winds transported smoke plumes toward the south, which is a prescribed fire approach sometimes called a backfire that is intended to maintain a slow rate of fire spread (Wade, 2013).

Figure 4. Satellite detected fires by the HMS system (dots) matched with November 13 (green) and 15 (yellow) burn units at Tallgrass Prairie for 2017. Picture, wind flow, fire progression, and ceilometer placement are shown for the November 15 prescribed burn.

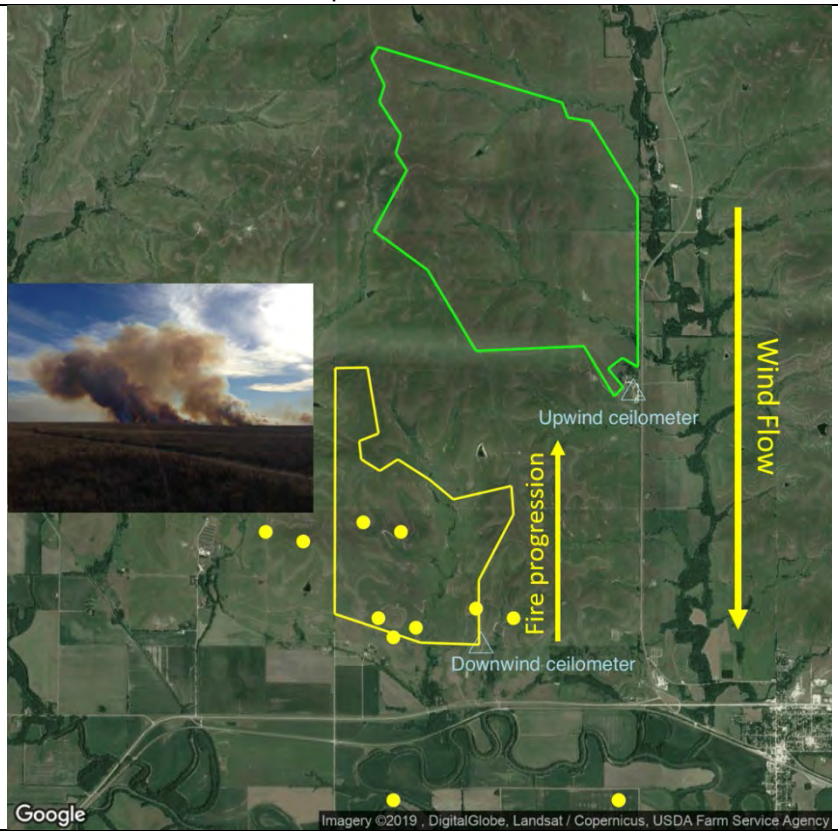

Smoke from the prescribed fire was evident in the ceilometer backscatter profile with near-ground plumes at the beginning of the burn when the fire was closest to the ceilometer (less than 1.5 km) to larger plumes that were sometimes decoupled from the surface toward the end of the burn when the fire was furthest (1.5 to 3.5 km) from the ceilometer (Figure 5). Smoke plumes extended from the surface to approximately 125 meters during the first half hour of the fire (12:35 to 1:15 pm), 250 meters during the next half hour (1:15 to 1:45 pm), and 500 meters between 1:45 and 2:15 pm. The smoke extended from the surface to top of the surface mixing layer at 2:30 and afterwards smoke was often

decoupled from the surface and plume heights were variable. Smoke plumes likely did not extend above the surface mixing layer at the ceilometer location, which may be due to the close proximity of the measurements to the fire activity. Most of the smoke plumes showed fairly uniform levels of aerosol backscatter from bottom to top and were rarely mixed from the surface to the top of the boundary layer.

Figure 5. Ceilometer profile of aerosol backscatter measured upwind (bottom panel) [AL1]and downwind (top panel) of the November 15, 2017 prescribed fire at Tallgrass Prairie. Ceilometer estimated surface mixing layer height (dashed line) also shown.

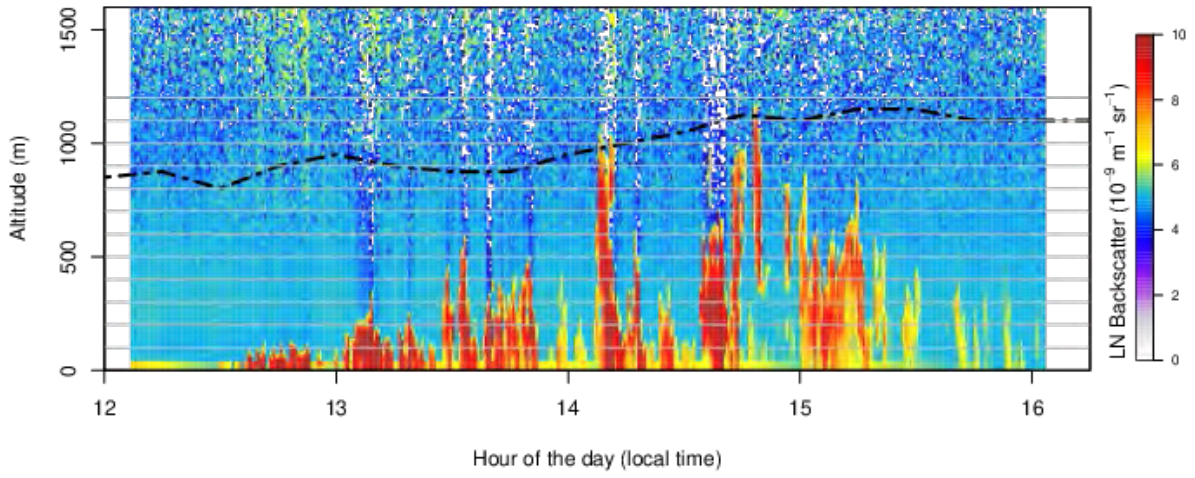

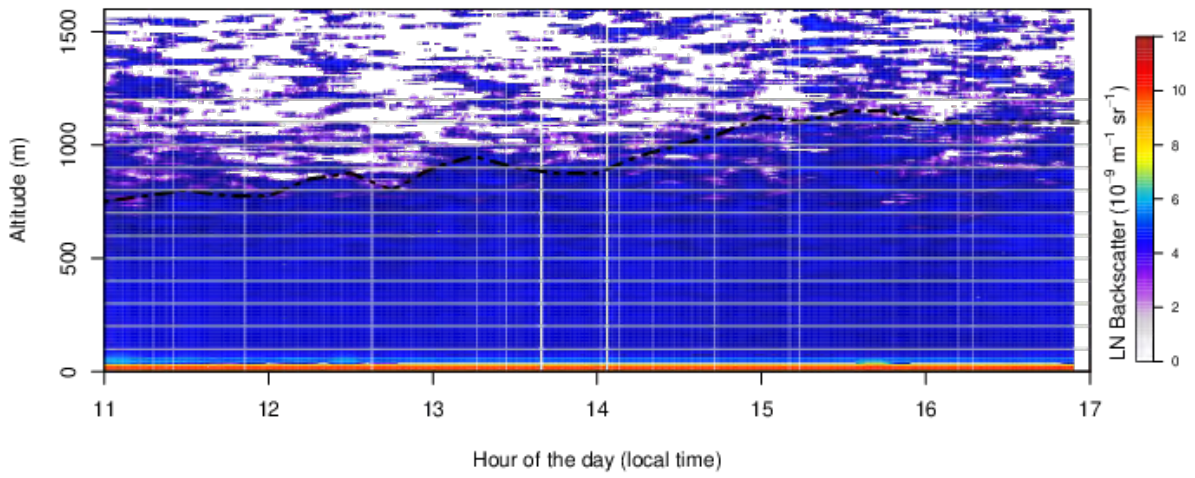

The 1 km model predicted plume from this prescribed fire is shown in Figure 6. The model provides hourly output that generally corresponds to the timing of the fire and estimates smoke plumes that are fairly well mixed from the surface to the top of the modeled boundary layer. The timing of the smoke from this fire starts too early and extends too late in the evening when the default temporal profile is used instead of actual timing information about the prescribed fire (Figure 6). Using the default profile results in very high surface concentrations in the early evening after the fire was over and places emissions in the free troposphere which will result in unrealistic downwind impacts locally and regionally.

Figure 6. November 15, 2017 prescribed fire $PM_{2.5}$ modeled at 1 km grid resolution using the actual start and end time (top) and the default temporal profile (bottom). Modeled planetary boundary layer height (solid line) and ceilometer estimated surface mixing layer height (dashed line) also shown.

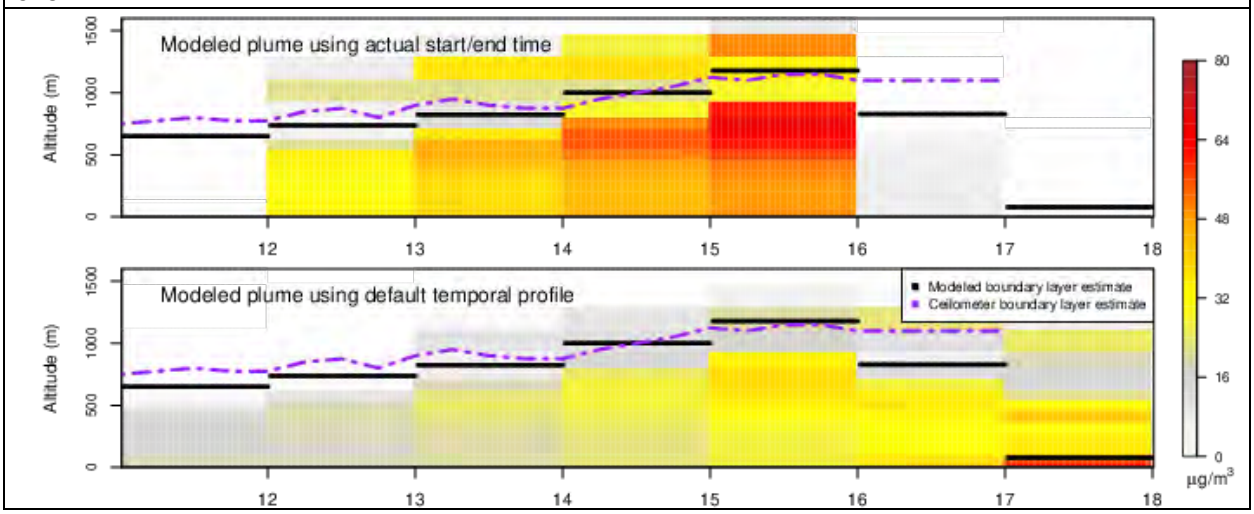

Since very little aerosol was present in the atmosphere, the smoke plumes provided the strongest vertical aerosol gradient which meant the ceilometer estimates of mixing layer height generally correspond to some part of the smoke plumes. The algorithm used by the ceilometer to estimate boundary layer tops sometimes correspond to plume edges, but often represented the middle of plumes while some of the densest plumes were not identified at all with the ceilometer mixing layer height algorithm (Figure A3).

March 16 and 17, 2017 case study

Prescribed fire impacts were modeled at the ceilometer location before dawn on March 16 from activity in southern Kansas and northeast Oklahoma late in the previous day (March 15). A 205 acre prescribed fire was set in the early afternoon at Konza Praire on March 16 and lasted until mid-afternoon (Table 2; burn 3). This fire was located to the southeast of the ceilometer location. Winds were steady from the south, which transported smoke from this prescribed fire to the north, but not directly toward the ceilometer (Figure 7). The model predicted some impacts from this prescribed fire at the ceilometer location when applied at 4 km resolution, but clear separation exists between the smoke plume and ceilometer location at 1 km resolution. Consistent with other studies (Baker et al., 2014), model prediction of peak impacts in the domain increased (usually at the source location) when these fires were modeled at finer grid resolution.

The modeling system shows impacts at the ceilometer location from prescribed fires at Konza Prairie on March 17, 2017. These modeled prescribed fires totaled approximately 30 acres and were set during the late afternoon to early evening time period. This prescribed fire was not included in the standard SmartFire2/BlueSky approach due to cloud cover, but also likely would not be detected due to the relatively small size and late in the day timing. Other prescribed fires in the region (located to the north) impacted the ceilometer location between noon and 6 pm. Agricultural tilling activity occurred in fields located immediately north of the ceilometer during March 17 and may have contributed brief periods of increased aerosol backscatter during the afternoon and evening (Figure 8). Afternoon elevated periods

of AOD were also observed at Konza Prairie and often match up to coincident increases in aerosol backscatter observed by the ceilometer.

Figure 7. Daily total forward trajectory weighted fire detections for March 16, 2017 (top left), modeled $PM_{2.5}$ from the prescribed fire at Konza Prairie at 1 pm local time (top right), photograph of the same prescribed fire at 2 pm local time taken from the east of the fire looking toward the northwest (bottom left), and vertical cross-sections of modeled $PM_{2.5}$ using actual and default timing information at the ceilometer location (bottom right).

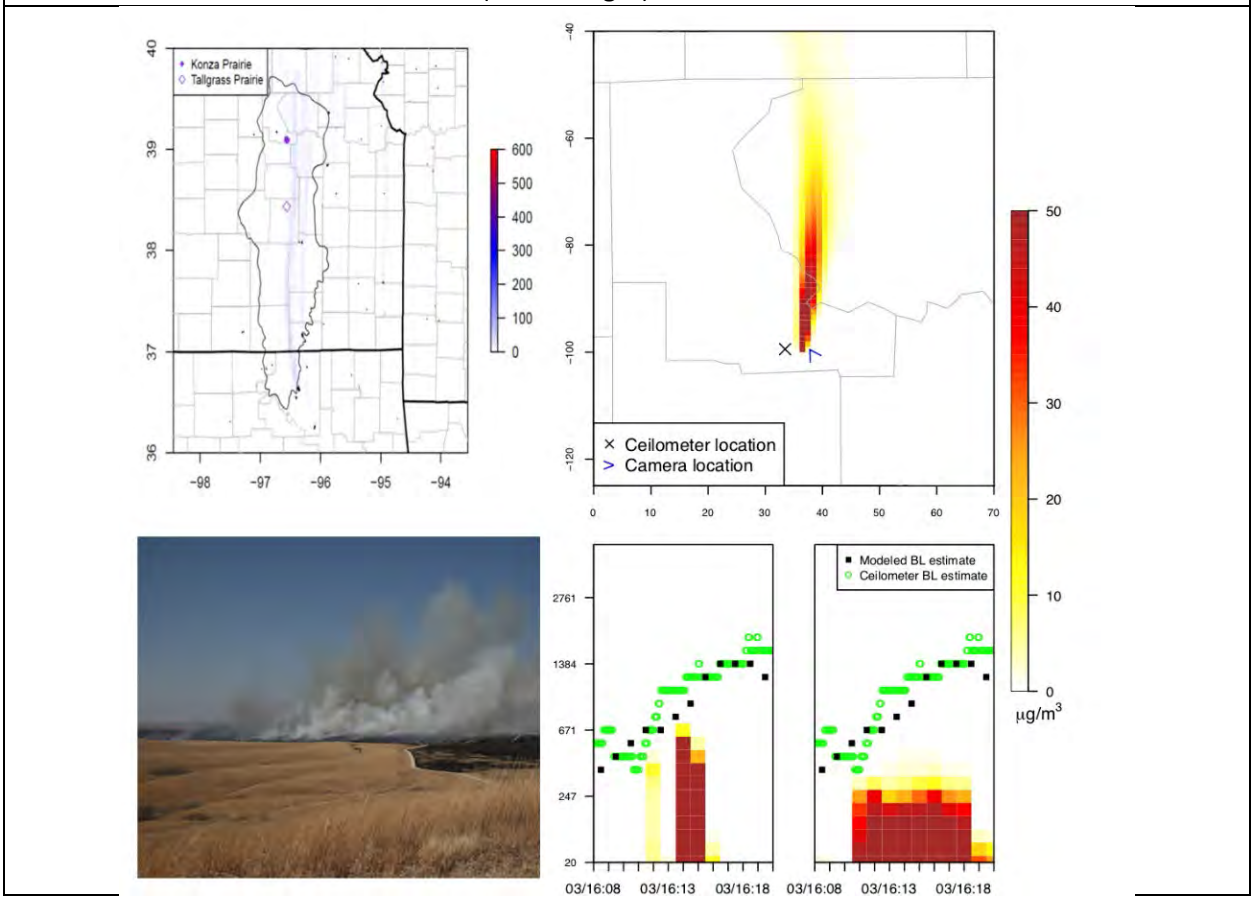

Figure 8. Aerosol backscatter measured by a ceilometer at Konza Prairie on March 17, 2017. Modeled planetary boundary layer height and ceilometer estimated surface layer mixing height (black) also shown. The grey box indicates the period and vertical extent of model predicted smoke impacts from prescribed fire. Agricultural tilling activity was observed upwind near the ceilometer on this day.

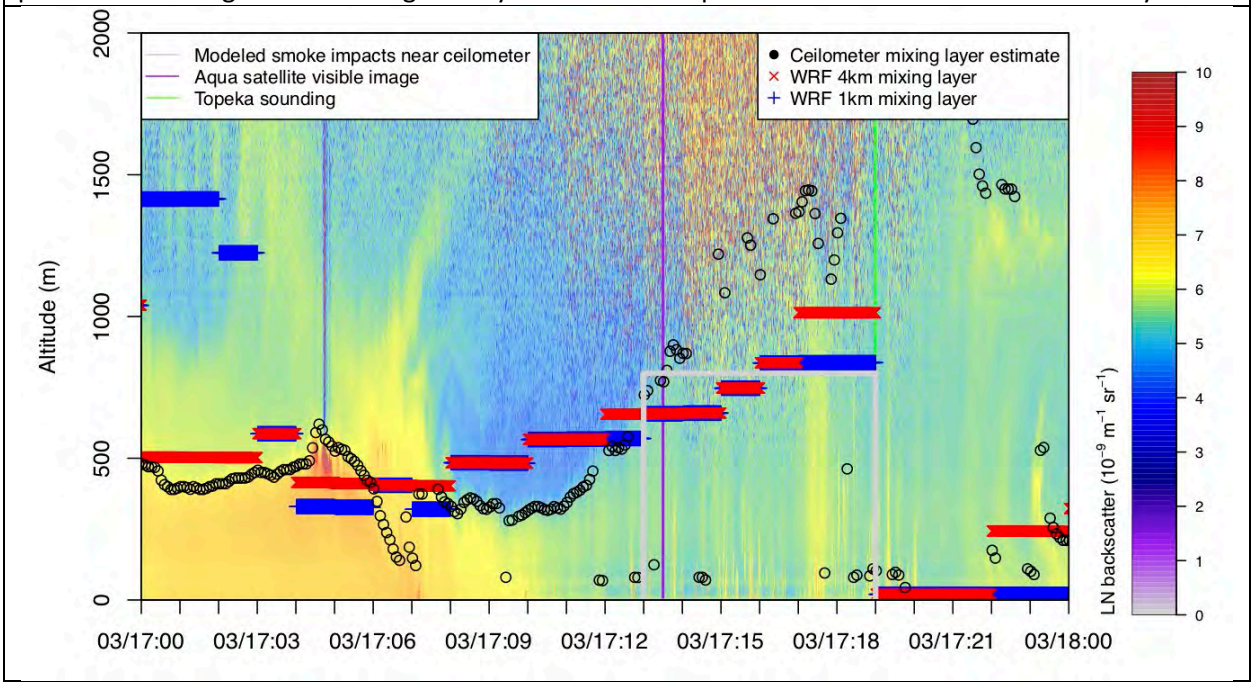

The smoke plume on March 16th was close to the ground at the flame front due to strong southerly winds consistently at ~15 mph and became well mixed through the boundary layer immediately downwind. Further downwind, smoke was evident toward the top of the surface mixing layer with less smoke near the surface. On March 17th, upper-level clouds and light northerly winds resulted in a stable plume updraft immediately over the location of active burning with the densest smoke nearest the surface and becoming less opaque as distance from the ground increased (Figure 9). When these prescribed fires were modeled with realistic timing information, the model did well to capture these plumes with a well-mixed plume on the 16th and a plume with highest concentration of smoke near the surface on the 17th of March (Figure 4 and 5). The prescribed fire plume is well mixed throughout the modeled surface mixing layer when using actual start and end times for the fire which results in higher estimated heat flux and higher plume rise compared to using the default temporal profile for prescribed fire.

Figure 9. Daily total forward trajectory weighted fire detections for March 17, 2017 (top left), modeled $PM_{2.5}$ from prescribed fires at 5 pm local time (top right), photograph of the Konza Prairie prescribed fire at 5 pm local time taken from the north of the fire looking toward the south (bottom left), and vertical cross-sections of modeled $PM_{2.5}$ using actual and default timing information at the ceilometer location (bottom right).

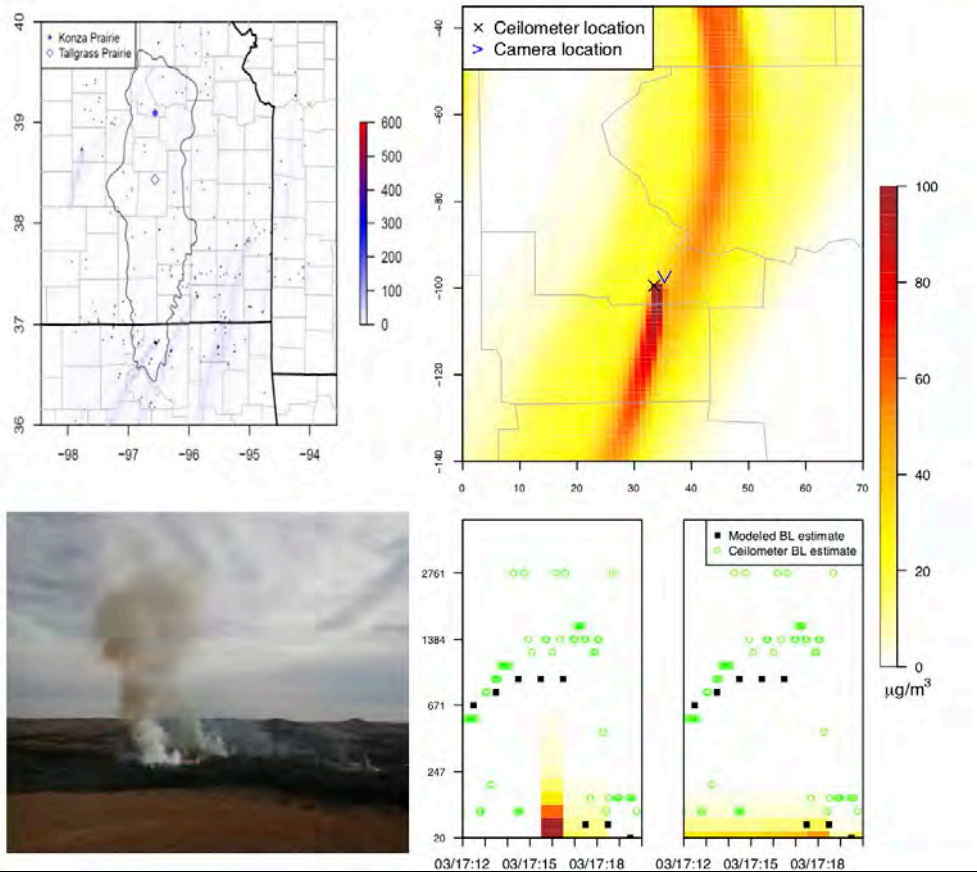

March 18, 2017 case study

Numerous prescribed fires were detected by satellite on March 18, 2017 and many were large enough to be seen with satellite imagery (Figure 10). As winds shifted from northerly to easterly during the day on March 18 and then southeasterly overnight smoke from afternoon prescribed fires to the north and east of Konza Prairie was transported to the ceilometer location. Smoke impacts persisted into the next morning (March 19). The modeling system shows a large impact of prescribed fire smoke during this period at the ceilometer location. The modeled impacts are well mixed from the surface through the surface mixing layer and up to clouds located about 2000 meters above ground level and generally coincide with the timing of elevated aerosol measured by the ceilometer. Vertical mixing is similar between the 12 and 4 km simulations. Regional smoke predictions were similar spatially between 12 and 4 km simulations but tended to be systematically lower at 12 km, especially near large isolated fires which is consistent with grid-based model system representation of primarily emitted pollutants (Baker et al., 2014).

Figure 10. March 18, 2017 modeled $PM_{2.5}$ from prescribed fires at 7 pm local time at 12 km resolution (left) and 4 km resolution (right).

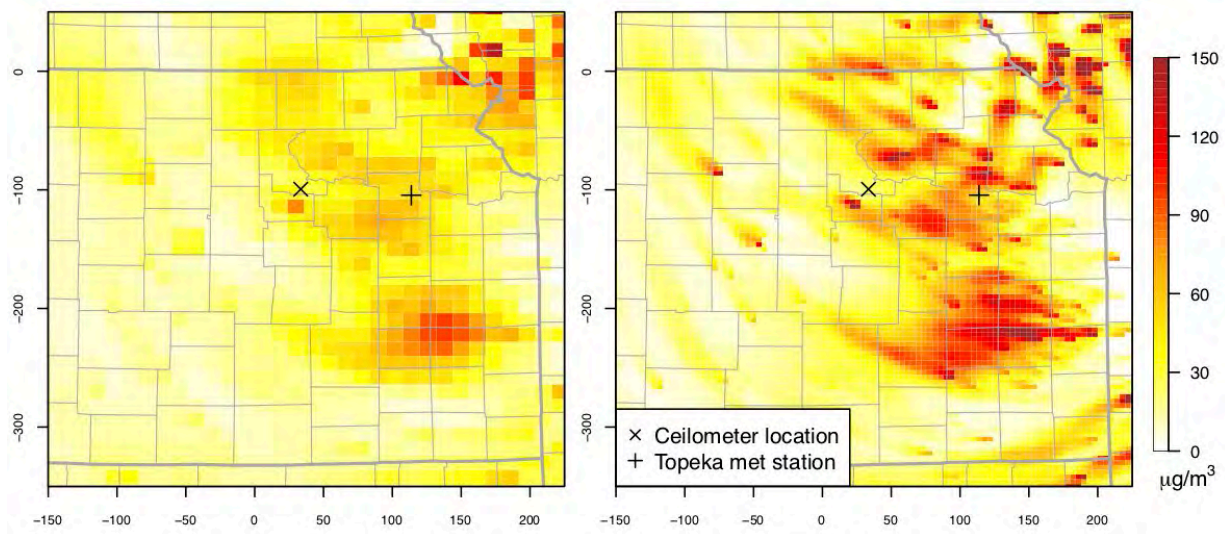

March 20, 2017 case study

Satellite imagery shows multiple prescribed fires near Konza Prairie on March 20, 2017 (Figure 11). An analysis of MODIS imagery burn scars from the prescribed fire complex to the northeast (Westmoreland) suggests these fires burned approximately 550 acres. The smoke plume from this complex and the prescribed fires at Konza Prairie are similar on visible images from the 1:30 pm Aqua satellite (Figure 11). Neither were visible on the 10:30 am terra satellite image meaning both started after the morning satellite overpass. The satellite image (Figure 11) of the Konza Prairie smoke plumes indicate a plume width of approximately 6 to 7 km downwind which compare well to the plume width predicted by the modeling system at 1 km resolution. The length of the Konza Prairie smoke plume on the satellite image is slightly longer than 40 km at 1:30 pm. This distance coupled with average winds of 20 km/hr suggest a start time between 11 and 11:30 am which matches well with the actual 10:45 am start time of the burn.

The Westmoreland complex plume width was approximately 3 km wide at 10 km downwind and 7 km wide at 20 km downwind. The full plume extent is difficult to discern on the satellite image but a 30 km total length with 20 km/hr winds suggests a start time around noon, which cannot be verified since those fires were not part of the field study. The modeling system predicts a plume width of approximately 4 to 7 km for the Westmoreland plume and suggest this fire and other regional prescribed fires impacted the ceilometer location.

Figure 11. March 20, 2017 true color satellite image from the aqua satellite at approximately 1 pm local time showing visible smoke plumes, fire detections, and clouds (left) and modeled $PM_{2.5}$ from the prescribed fires at 1 pm local time (right).

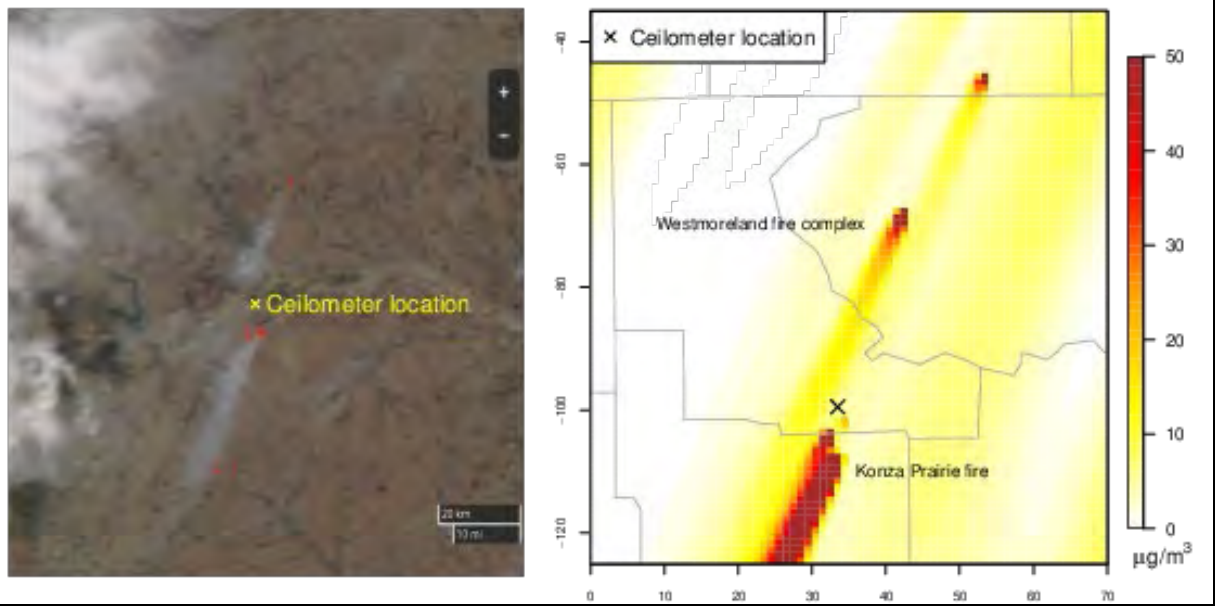

Local to Regional Scale Transport

Modeling system skill in representing local to regional scale plume transport of $PM_{2.5}$ depends on many variables, most notably meteorology. Modeled winds and temperature at the surface and aloft were compared to routine measurements to evaluate smoke transport. Table 3 shows aggregated model performance metrics over all monitors in the model domain for temperature, water mixing ratio, wind speed, and wind direction for the spring and fall time periods. Aggregate performance for temperature (mean error < 2 degrees K) and water mixing ratio (mean error < 1 g/kg) at both grid resolutions and seasons was comparable to other continental scale WRF simulations (US EPA, 2011; UNC, 2015). Winds were slightly over-predicted (mean bias between 1.5 and 1.75 mph) compared to observation data (Table 3) and slightly worse than aggregate continental scale WRF performance shown in other studies (US EPA, 2011; UNC, 2015).

The model does well in both seasons capturing synoptic and diurnal variability of solar radiation, temperature, wind speed, and wind direction at Tallgrass Prairie (Figures A4 and A5). Daytime solar radiation is well characterized but the model tends to under-estimate solar radiation on cloudy days (Figures A4 and A5). The model did well replicating temperature, wind speed, and wind direction during periods of increased prescribed fire activity (Figure A4 and A5).

Table 3. Aggregate model performance metrics for routine surface measurements and model predictions from the 4 and 1 km WRF simulations.

	Spring		November	
	4km	**1km**	**4km**	**1km**
# of sites	330	3	330	9
# of hourly model prediction-observation pairings	456,256	4,243	28,346	2,112
2m Temperature Mean Bias (K)	-0.4	-0.17	-0.4	-0.45
2m Temperature Error (K)	1.65	1.71	1.47	1.5
2m Mixing Ratio Bias (g/kg)	0.22	0.37	0.18	-0.24
2m Mixing Ratio Error (g/kg)	0.73	0.7	0.53	0.56
10m Wind Speed Bias (m/s)	0.71	0.71	0.78	0.68
10m Wind Speed RMSE	1.87	1.85	1.66	1.5
10m Wind Direction Bias (°)	4.7	-0.75	4.52	1.1
10m Wind Direction Error (°)	19.43	19.14	15.82	16.2

Model predicted surface boundary layer heights generally follow synoptic and diurnal patterns estimated by the BL-view software (Figure 12 and 8). However, WRF often predicted a nocturnal stable layer (NSL) that was much closer to the surface which BL-View was unable to detect from the ceilometer backscatter profile (Figures 3 and S4). The inability of the ceilometer to resolve this feature of the NSL may be the result of low aerosol content (i.e. clean conditions) in the NSL or that WRF is predicting the NSL too close to the surface. However, the ceilometer did appear to capture the residual aerosol layer during the night and day time hours above the NSL and convective boundary layer.

Figure 12. Aerosol backscatter measured by a ceilometer at Konza Prairie during November 2017. Modeled planetary boundary layer height and ceilometer estimated surface layer mixing height (black) also shown. Models and data do not suggest prescribed grassland fire impacts during this period.

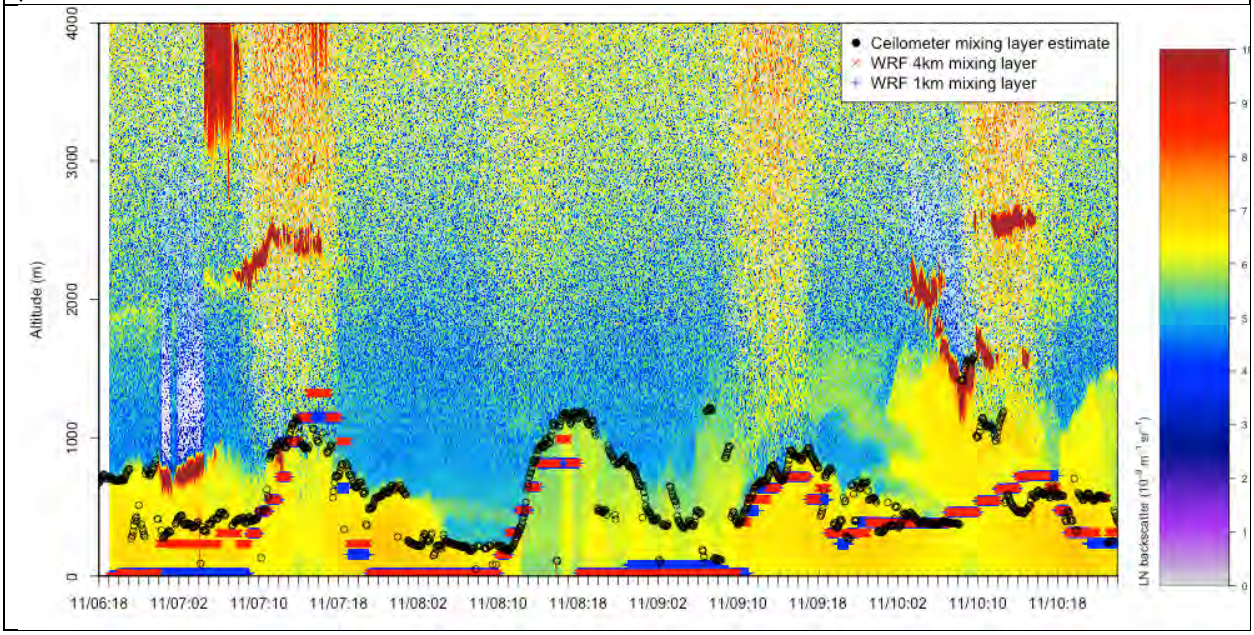

4. CONCLUSIONS, CURRENT AND FUTURE WORK

Accurate representation of surface and aloft winds and smoke plume size compared with visible satellite images suggest the modeling system shows skill toward capturing local to regional scale smoke plume transport from prescribed grassland fire. The use of more realistic start and end times for prescribed fire resulted in a better match against smoke plumes measured with a ceilometer. Within day timing can to some degree be approximated based on total acres burned and where available improved with accurate fuel consumption information. Cloudy conditions and smaller prescribed fires outside the timing of polar orbiting satellites result in small fires not being captured in the modeling system. A simple prescribed fire tracking system linking burn unit specific information (e.g., area burned, fuel types, and fuel loading), day of the burn, and approximate start and end times would be valuable toward better representation of prescribed grassland fires in air quality modeling systems. Predicted O_3 impacts were higher in March compared to November for a prescribed fire with identical size and emissions both locally and regionally while $PM_{2.5}$ impacts were comparable regionally, which is generally consistent with weather being more O_3 conducive during the March period. However, additional work is needed to understand how well the modeling system characterizes the chemical evolution of secondarily formed pollutants in grassland fire plumes from the fire location to regional scales. Further, more studies are needed comparing air quality impacts of prescribed grassland fires in this region during different times of year.

This report of the 2017 field study in the Flint Hills has provided a basis for the tools and techniques available to further analyze the prescribe burning and smoke impact in Eastern Kansas. A limitation to the 2017 study was the limited timeframe that the ceilometer was deployed, and thus it did not provide an ideal dataset of the prescribed burning throughout the predominate burn period (i.e., early April). Since the 2017 field study, a Vaisala CL-51 ceilometer has permanently been placed at Konza Prairie (https://alg.umbc.edu/kpks-archive-calendar/). It has been in operation since March of 2020 and has provided data and visualization for two springtime Flint Hills prescribed burn seasons (2020 and 2021), along with showing smoke transport from Western U.S. wildfires in the summer of 2020 and long-range transport of Saharan dust from west Africa. The type details provided by the Konza Prairie ceilometer are highlighted in Figure 13 and Figure 14.

Figure 13 shows the ceilometer backscatter during the March 31, 2020 Flint Hills prescribed burn event. Smoke from burning is seen on the backscatter and the evolution of the daytime mixed layer is evident, with smoke being mixed within the growing afternoon planetary boundary layer. The ceilometer shows the destruction of the daytime mixed layer and the transition to the more stratified nighttime boundary (between 1:00 and 3:00 UTC). Figure 14 shows that most of the smoke from daytime burning sits above the nighttime boundary layer, detached from the surface. Also evident is smoke from evening or nighttime burning that is “trapped” within the stable nighttime boundary (3:00 UTC).

Figure 13. Aerosol backscatter from the CL-51 ceilometer at Konza Prairie showing smoke during a prescribed fire event on March 31, 2020.

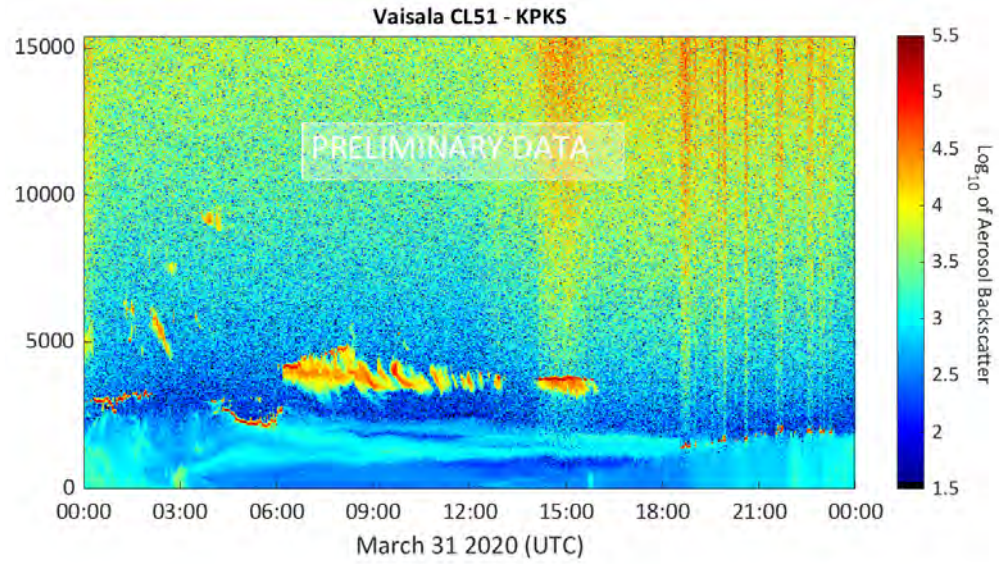

Figure 14 provides an example of the transport of long-range smoke from wildfires from the Western U.S. The September 18, 2020 ceilometer backscatter indicates an atmospheric layer of smoke between 1,000 and 3,000 meters above the surface. The smoke layer tends to be transported within the free atmosphere above the boundary layer, limiting the smoke impact on the surface. The daytime heating may be able to mix the smoke within the afternoon boundary layer starting at 21:00 UTC.

Figure 14. Aerosol backscatter from the CL-51 ceilometer at Konza Prairie showing the Western U.S. smoke transport on September 18, 2020.

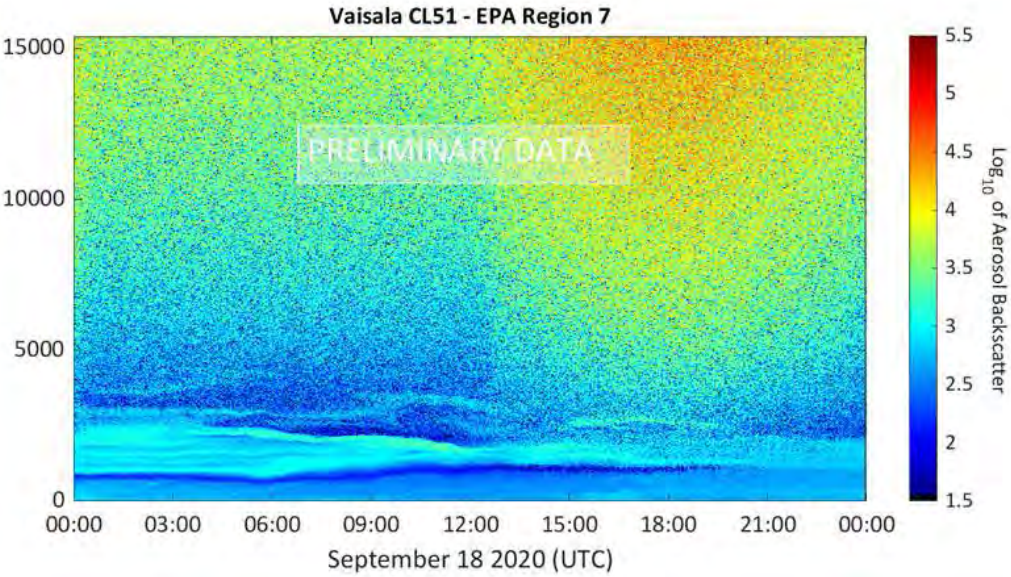

In March of 2020, a Pandora ground-based spectrometer Pandora was installed at Konza Prairie (Figure 15). Pandora provides high-quality spectrally resolved direct sun/lunar or sky scan radiance measurements in the UV and visible wavelengths. The Pandora radiance measurements provide real-time data of key air quality relevant pollutants, which can be compared to similar measurements from satellites. These observations include total column O_3, NO_2, and formaldehyde (HCHO).

Figure 15. The Pandora spectrometer located at Konza Prairie.

Pandora column NO_2 combined with the ceilometer vertical aerosol backscatter and mixed layer height measurements will aid in the characterization of prescribed burning in the Flint Hills Region. By capturing the total column of pollution as opposed to routine surface measurements, Pandora can better track local to regional scale smoke plumes, especially when the smoke is decoupled from the surface. The Pandora is also valuable for direct comparison with satellite based NO_2 column measurements to validate and improve retrievals for unique areas like the central U.S. where prescribed burning provides an episode large NO_2 signal compared to relatively sparse emissions sources nearby. This data collected at Konza Prairie site from the Pandora and ceilometer will further aid in the development, validation, and use of the air quality modeling system that are described in this Report. These include but are not limited to: model profile of fire timing and duration, modeled vertical plume height, modeled secondary chemistry for prescribed burning, and the air quality impacts of prescribed fires during different seasons (i.e., a spring vs fall burn).

Contributors to this report

Kirk Baker, Lance Avey, Andy Hawkins , Lara Reynolds, Chris Allen, Barron Henderson, Brian Gullett, Amara Holder, Matt Landis, Russell Long, George Pouliot, Jeff Vukovich, Venkatesh Rao, Norm Possiel, Chris Misenis, Nathaniel Bunsell, Joe Wilkins, and Patrick O'Neal.

Disclaimer

The views expressed in this article are those of the authors and do not necessarily represent the views or policies of the U.S. Environmental Protection Agency.

REFERENCES

Baker, K., Koplitz, S., Foley, K., Avey, L., Hawkins, A., 2019. Characterizing grassland fire activity in the Flint Hills region and air quality using satellite and routine surface monitor data. Science of The Total Environment 659, 11.

Baker, K., Woody, M., Tonnesen, G., Hutzell, W., Pye, H., Beaver, M., Pouliot, G., Pierce, T., 2016. Contribution of regional-scale fire events to ozone and PM 2.5 air quality estimated by photochemical modeling approaches. Atmospheric Environment 140, 539-554.

Baker, K., Woody, M., Valin, L., Szykman, J., Yates, E., Iraci, L., Choi, H., Soja, A., Koplitz, S., Zhou, L., 2018. Photochemical model evaluation of 2013 California wild fire air quality impacts using surface, aircraft, and satellite data. Science of The Total Environment 637, 1137-1149.

Baker, K.R., Hawkins, A., Kelly, J.T., 2014. Photochemical grid model performance with varying horizontal grid resolution and sub-grid plume treatment for the Martins Creek near-field SO 2 study. Atmospheric Environment 99, 148-158.

Brey, S.J., Ruminski, M., Atwood, S.A., Fischer, E.V., 2017. Connecting smoke plumes to sources using Hazard Mapping System (HMS) smoke and fire location data over North America. Atmos. Chem. Phys. Discuss., https://doi. org/10.5194/acp-2017-245, in review.

Carlton, A.G., Bhave, P.V., Napelenok, S.L., Edney, E.O., Sarwar, G., Pinder, R.W., Pouliot, G.A., Houyoux, M., 2010. Treatment of secondary organic aerosol in CMAQv4.7. Environmental Science and Technology 44, 8553-8560.

Emery, C., Jung, J., Koo, B., Yarwood, G., 2015. Improvements to CAMx Snow Cover Treatments and Carbon Bond Chemical Mechanism for Winter Ozone. Prepared for the Utah Department of Environmental Quality, Division of Air Quality, Salt Lake City, UT. Available at: http://www.camx.com/files/udaq_snowchem_final_6aug15.pdf.

Fahey, K.M., Carlton, A.G., Pye, H.O., Baek, J., Hutzell, W.T., Stanier, C.O., Baker, K.R., Appel, K.W., Jaoui, M., Offenberg, J.H., 2017. A framework for expanding aqueous chemistry in the Community Multiscale Air Quality (CMAQ) model version 5.1. Geoscientific Model Development 10.

Fountoukis, C., Nenes, A., 2007. ISORROPIA II: a computationally efficient thermodynamic equilibrium model for K+-Ca2+-Mg2+-Nh(4)(+)-Na+-SO42--NO3--Cl--H2O aerosols. Atmospheric Chemistry and Physics 7, 4639-4659.

Iacono, M.J., Delamere, J.S., Mlawer, E.J., Shephard, M.W., Clough, S.A., Collins, W.D., 2008. Radiative forcing by long-lived greenhouse gases: Calculations with the AER radiative transfer models. Journal of Geophysical Research: Atmospheres 113.

Kansas Department of Health and Environment, 2010. State of Kansas Flint Hills Smoke Management Plan December, 2010. http://www.ksfire.org/docs/about/Flint_Hills_SMP_v10FINAL.pdf.

Kansas Department of Health and Environment, 2012. State of Kansas Exceptional Event Demonstration Package April 6, 12, 13, and 29, 2011. Department of Health and Environment, Division of Environment, Bureau of Air. November 27, 2012. http://www.epa.gov/ttn/analysis/docs/KDHE_ExEvents_final_042011.pdf.

Kelly, J.T., Baker, K.R., Napelenok, S.L., Roselle, S.J., 2015. Examining single-source secondary impacts estimated from brute-force, decoupled direct method, and advanced plume treatment approaches. Atmospheric Environment 111, 10-19.

Knepp, T.N., Szykman, J.J., Long, R., Duvall, R.M., Krug, J., Beaver, M., Cavender, K., Kronmiller, K., Wheeler, M., Delgado, R., 2017. Assessment of mixed-layer height estimation from single-wavelength ceilometer profiles. Atmospheric measurement techniques 10, 3963.

Larkin, N.K., Raffuse, S.M., Strand, T.M., 2014. Wildland fire emissions, carbon, and climate: US emissions inventories. Forest Ecology and Management 317, 61-69.

Niu, G.Y., Yang, Z.L., Mitchell, K.E., Chen, F., Ek, M.B., Barlage, M., Kumar, A., Manning, K., Niyogi, D., Rosero, E., 2011. The community Noah land surface model with multiparameterization options (Noah-MP): 1. Model description and evaluation with local-scale measurements. Journal of Geophysical Research: Atmospheres 116.

Ratajczak, Z., Briggs, J.M., Goodin, D.G., Luo, L., Mohler, R.L., Nippert, J.B., Obermeyer, B., 2016. Assessing the potential for transitions from tallgrass prairie to woodlands: are we operating beyond critical fire thresholds? Rangeland Ecology & Management 69, 280-287.

Reid, C.E., Brauer, M., Johnston, F.H., Jerrett, M., Balmes, J.R., Elliott, C.T., 2016. Critical review of health impacts of wildfire smoke exposure. Environmental Health Perspectives 124, 1334-1343.

Skamarock, W.C., Klemp, J.B., Dudhia, J., Gill, D.O., Barker, D.M., Wang, W., Powers, J.G., 2005. A description of the advanced research WRF version 2. National Center For Atmospheric Research Boulder Co Mesoscale and Microscale ….

Thompson, G., Field, P.R., Rasmussen, R.M., Hall, W.D., 2008. Explicit forecasts of winter precipitation using an improved bulk microphysics scheme. Part II: Implementation of a new snow parameterization. Monthly Weather Review 136, 5095-5115.

Tiedtke, M., 1989. A comprehensive mass flux scheme for cumulus parameterization in large-scale models. Monthly Weather Review 117, 1779-1800.

Towne, E.G., Craine, J.M., 2016. A critical examination of timing of burning in the Kansas Flint Hills. Rangeland ecology & management 69, 28-34.

Wade, D., 2013. Backfire technique for prescribed burning. http://www.southernfireexchange.org/SFE_Publications/factsheets/2013_2.pdf. Accessed July 2019. .

Wagstrom, K.M., Baker, K.R., Leinbach, A.E., Hunt, S.W., 2014. Synthesizing Scientific Progress: Outcomes from US EPA's Carbonaceous Aerosols and Source Apportionment STAR Grants. Environmental science & technology 48, 10561-10570.

Washenfelder, R.A., Azzarello, L., Franchin, A., Middlebrook, A.M., 2019. Brown Carbon Aerosol Absorption in Western Wildfires, AGU Fall Meeting 2019. AGU.

Weir, J.R., Scasta, J.D., 2017. Vegetation responses to season of fire in tallgrass prairie: a 13-year case study. Fire Ecology 13, 137-142.

Whitehill, A.R., George, I., Long, R., Baker, K.R., Landis, M., 2019. Volatile Organic Compound Emissions from Prescribed Burning in Tallgrass Prairie Ecosystems. Atmosphere 10, 464.

Zhou, L., Baker, K.R., Napelenok, S.L., Pouliot, G., Elleman, R., O'Neill, S.M., Urbanski, S.P., Wong, D.C., 2018. Modeling crop residue burning experiments to evaluate smoke emissions and plume transport. Science of The Total Environment 627, 523-533.

APPENDIX A

Figure A1. Temporal profile used to allocate daily wildland (wild and prescribed) fire emissions to specific hours of the day.

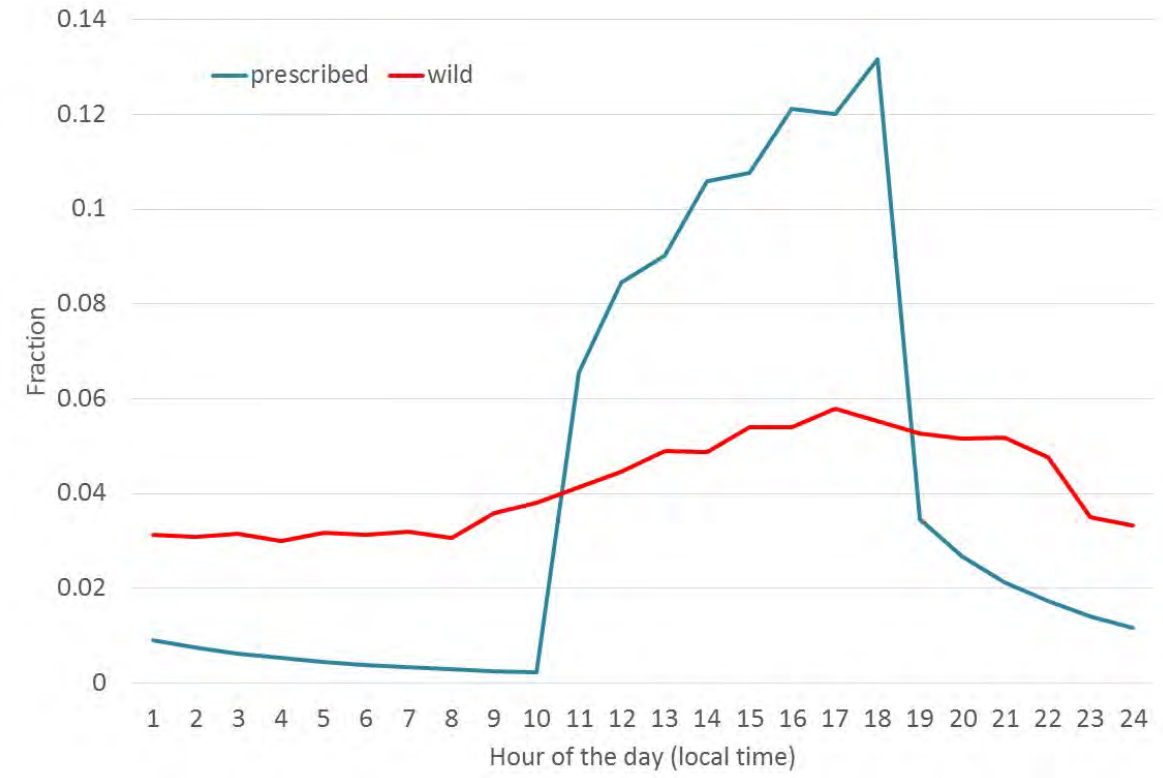

Figure A2. Satellite detected fires based on the HMS system (red) and burn areas (green outline) by day at Konza Prairie (blue outline) for 2018. Gray shading represents grassland coverage at 1 km grid spacing.

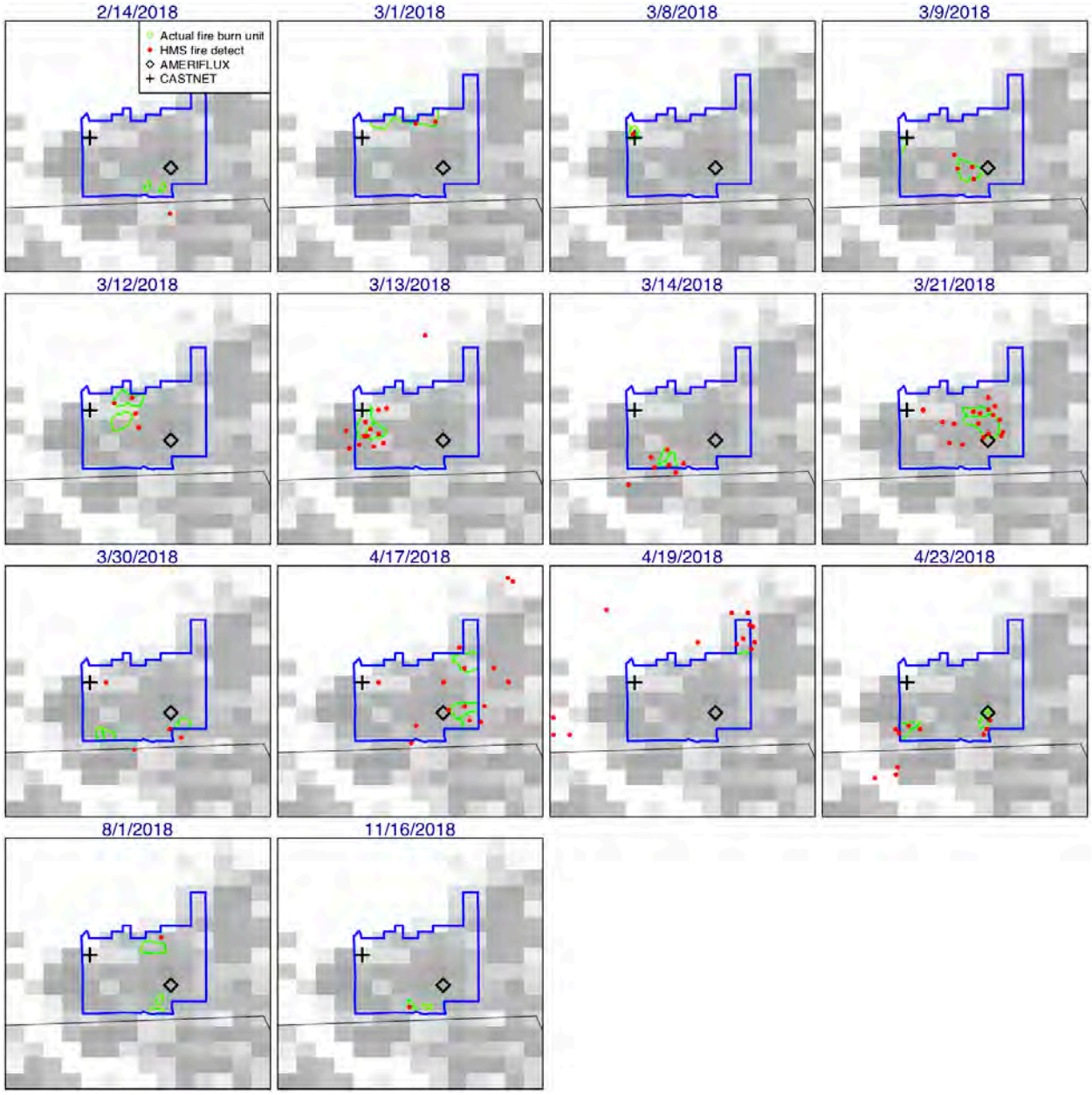

Figure A3. Ceilometer profile of aerosol backscatter measured upwind and downwind of a prescribed fire at Tallgrass Prairie in 2017 (top). The same prescribed fire $PM_{2.5}$ modeled at 1 km grid resolution using the actual start and end time and the default temporal profile.

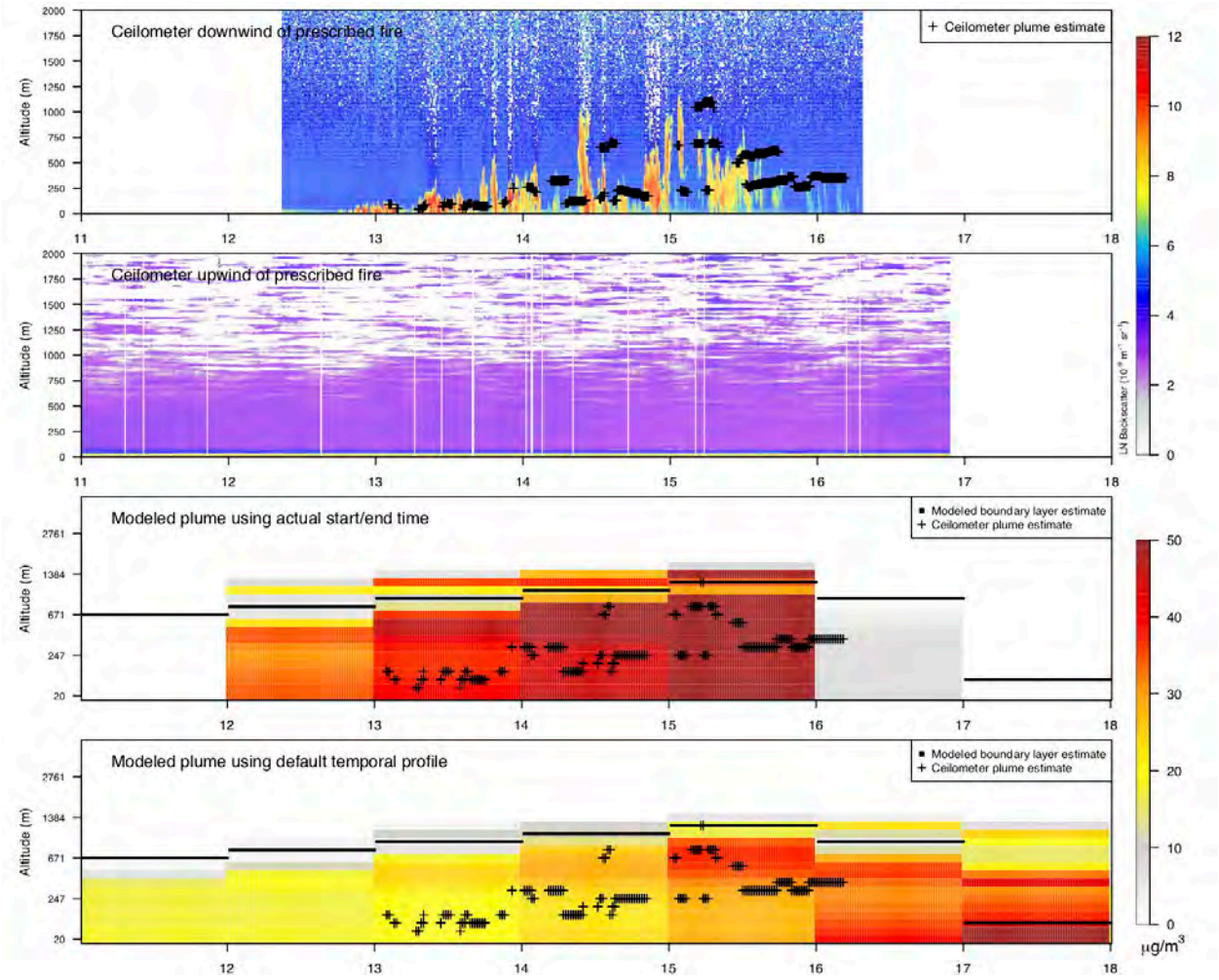

Figure A4. Observations and model predictions (local time) at Tallgrass Prairie for a period of March 2017. Measured fuel moisture is also shown. HMS fire detections are shown in the top panel based on fire radiative power when that data was provided and simply as a detection (orange square) for detections without fire radiative power information.

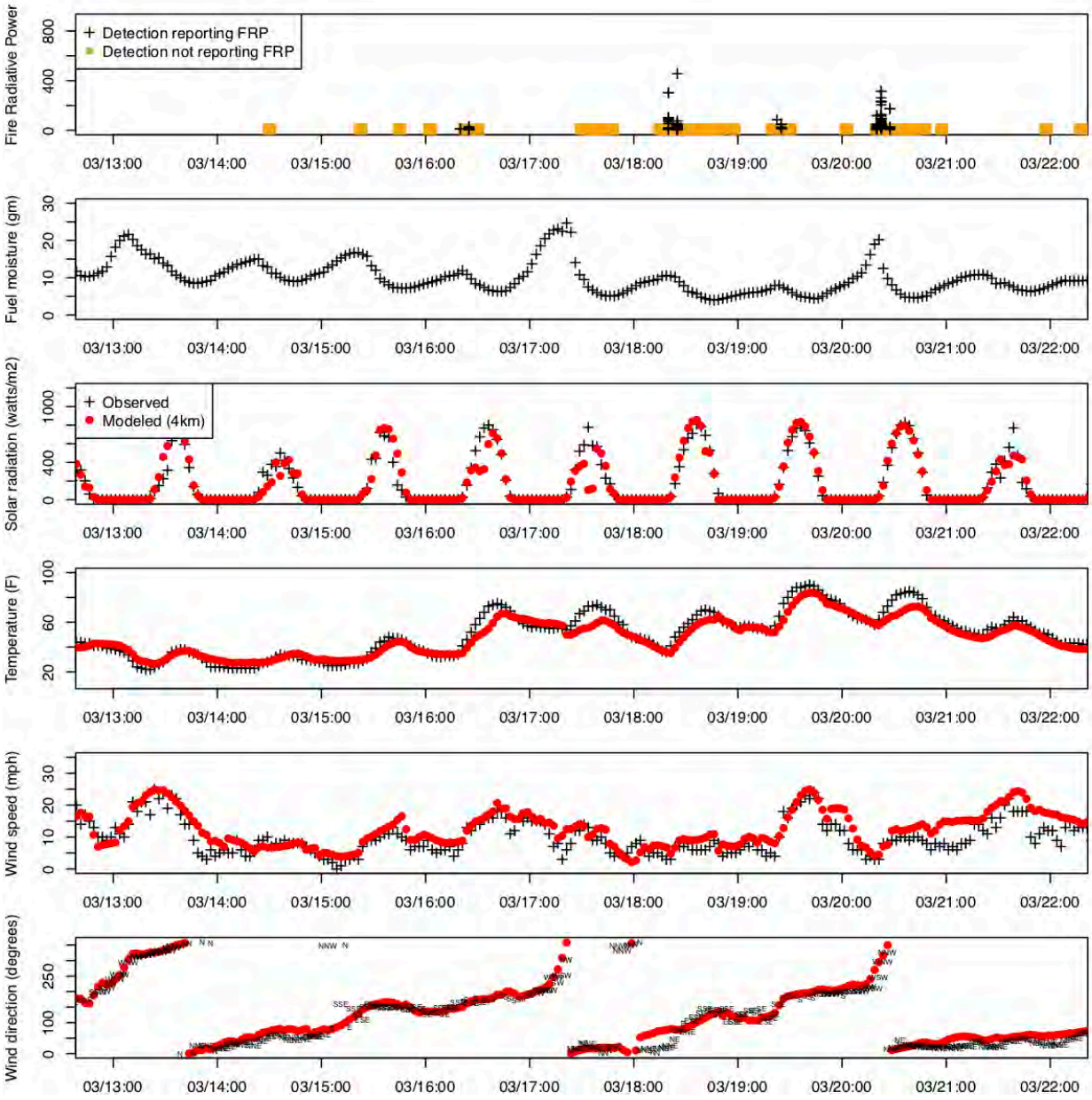

Figure A5. Observations and model predictions (local time) at Tallgrass Prairie for a period of November 2017. Measured fuel moisture is also shown. HMS fire detections are shown in the top panel based on fire radiative power when that data was provided and simply as a detection (orange square) for detections without fire radiative power information.

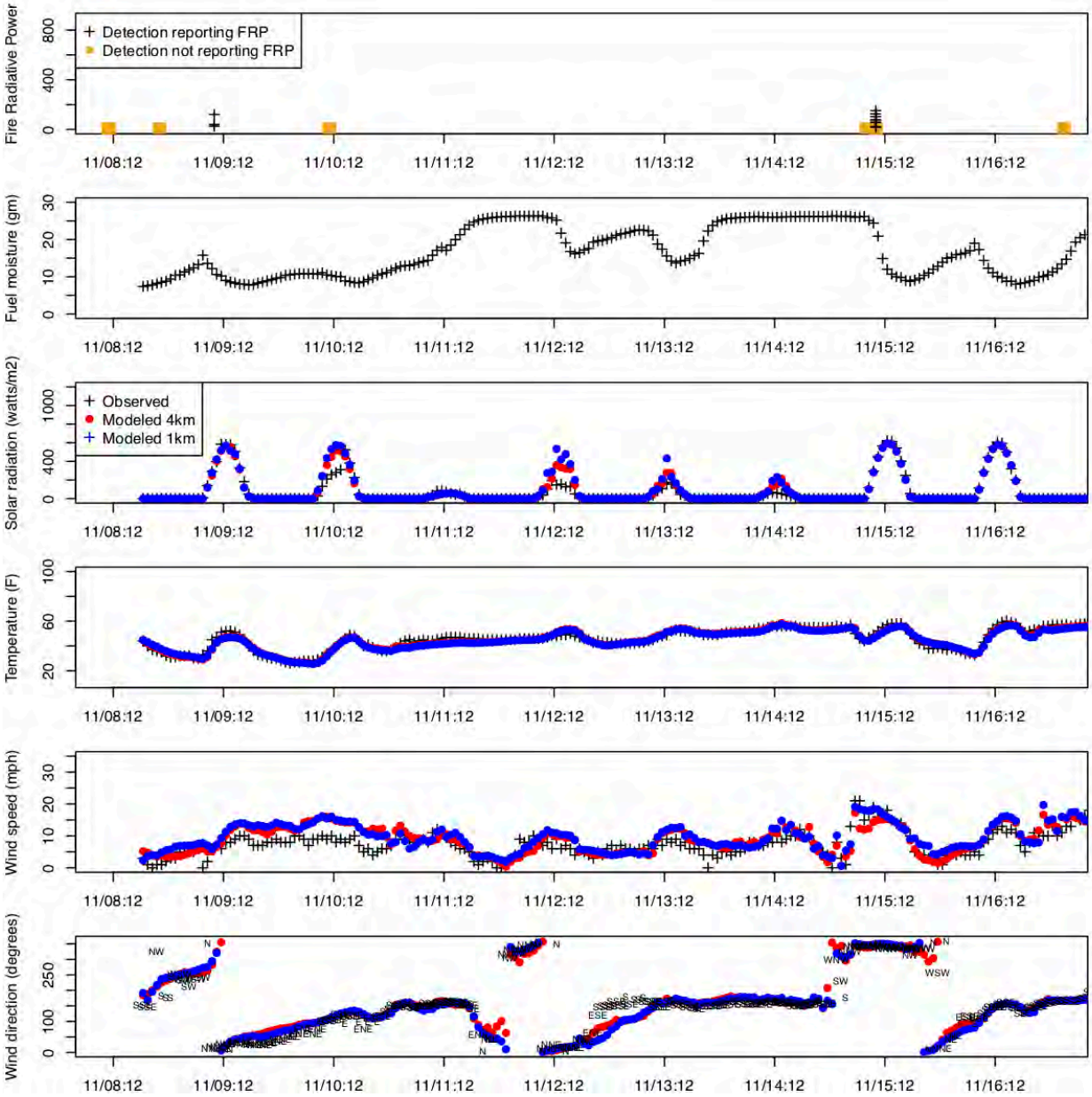

Figure A6. The distribution of temperature, wind speed, solar radiation, and fuel moisture made at Tallgrass Prairie by month for the years 2002 to 2018. The solar radiation panel only includes data collected between 8 am and 8 pm.

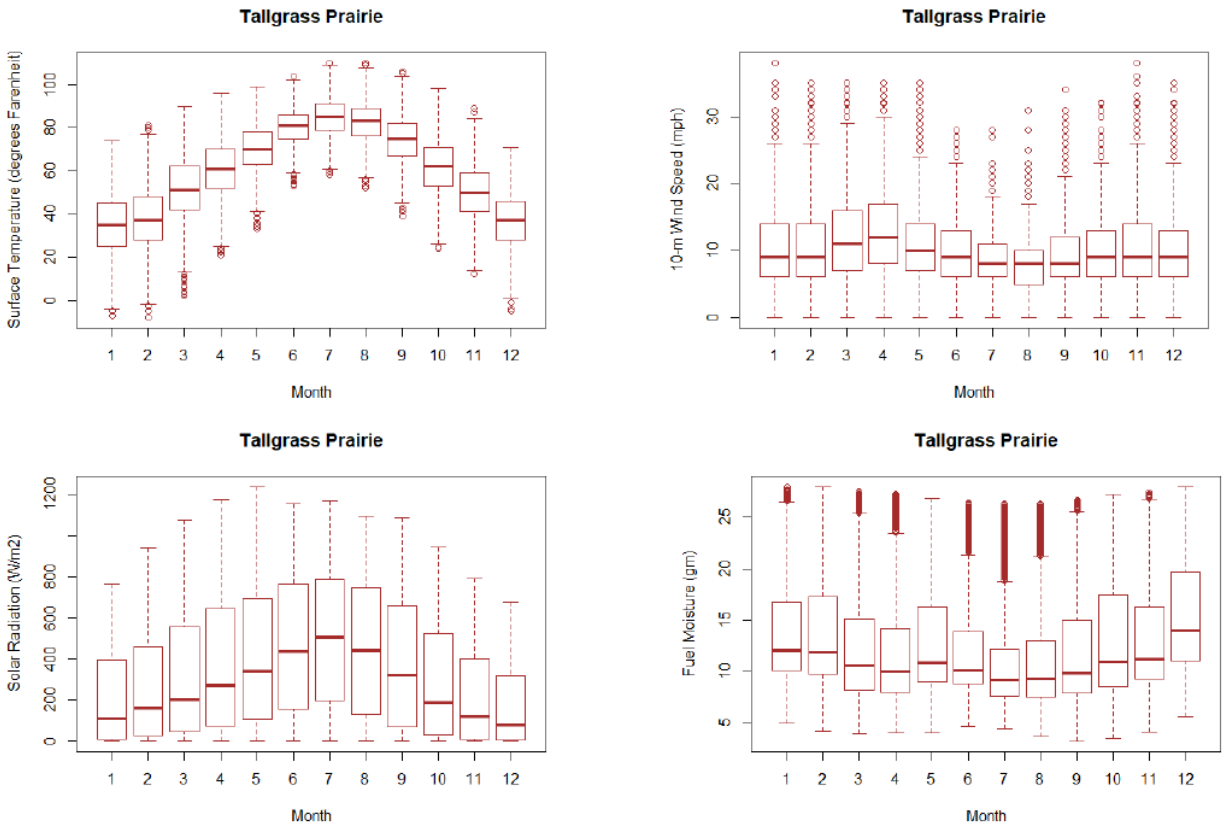

APPENDIX B

Images from each of the prescribed burns at Konza Prairie and Tallgrass Prairie in 2017.


March 16, 2017 Konza Prairie


November 10, 2017 Konza Prairie


March 17, 2017 Konza Prairie


November 13, 2017 Tallgrass Prairie


March 20, 2017 Konza Prairie


November 15, 2017 Tallgrass Prairie

United States Environmental Protection Agency	Office of Air Quality Planning and Standards Air Quality Assessment Division Research Triangle Park, NC	Publication No. EPA-454/R-21-004 June 2021